Ultrasound-Mediated Transscleral Delivery of Macromolecules to the Posterior Segment of Rabbit Eye In Vivo

Wai-Leung Langston Suen,[1] Hoi Sang Wong,[1] Yu Yu,[2] Laurence Chi Ming Lau,[3] Amy Cheuk-Yin Lo,[3] and Ying Chau[1,2]

[1]Department of Chemical and Biomolecular Engineering, The Hong Kong University of Science and Technology, Clear Water Bay, Kowloon, Hong Kong, China
[2]Division of Biomedical Engineering, The Hong Kong University of Science and Technology, Clear Water Bay, Kowloon, Hong Kong, China
[3]Department of Ophthalmology, The University of Hong Kong, Pok Fu Lam, Hong Kong, China

Correspondence: Ying Chau, The Hong Kong University of Science and Technology, Clear Water Bay, Kowloon, Hong Kong, China; keychau@ust.hk.

Submitted: March 5, 2013
Accepted: May 21, 2013

Citation: Suen W-LL, Wong HS, Yu Y, Lau LCM, Lo AC-Y, Chau Y. Ultrasound-mediated transscleral delivery of macromolecules to the posterior segment of rabbit eye in vivo. *Invest Ophthalmol Vis Sci*. 2013;56:4358–4365. DOI:10.1167/iovs.13-11978

Purpose. This study aims to determine the in vivo effectiveness of low-frequency ultrasound in mediating the transport of macromolecules to the posterior segment of the eye via transscleral route. It investigates if damage is caused by ultrasound at the tested operation parameters on the posterior ocular tissues and visual function.

Methods. Ultrasound (I_{SATA} = 0.12 W/cm^2, center frequency = 40 kHz, 90-second continuous wave) was applied on the sclera of New Zealand white rabbits for one to three cycles. Solution of fluorescent dextran (70 kDa) was placed above sclera during and after ultrasound application to assess transscleral transport of macromolecules. Amount of dextran delivered to vitreous was determined by detection of fluorescence. Visual function of ultrasound-treated rabbits was examined by full-field electroretinography (ffERG). The effect of ultrasound on ocular tissue structures was examined by binocular indirect ophthalmoscope (BIO) and histology.

Results. Repeated ultrasound resulted in increasing concentration of dextran, which was otherwise undetectable in the vitreous. Transscleral barrier against dextran transport was restored to original value at 2 weeks postultrasound treatment. Studies from ffERG suggested that electric responses from neural transmission of retinal cells are normal at 1 day, 7 days, and 14 days after ultrasound applications. BIO and histology revealed no structural abnormality in posterior ocular tissues after ultrasound treatment.

Conclusions. Low-frequency ultrasound significantly enhanced the penetration of macromolecules via transscleral route. No undesirable side effects have been found for up to 2 weeks after ultrasound application. The study supports that sonication is a potentially safe and effective method to modulate transscleral barriers for delivering macromolecular therapeutics to posterior segment of the eye.

Keywords: needleless, noninvasive, ocular delivery, retinal disease

Posterior eye diseases, such as age-related macular degeneration, can lead to impaired vision and blindness. This has become an increasing healthcare burden on the aging society.[1] New and emerging therapeutics are mostly biomacromolecules, which do not readily enter the eye.[2–7] Current clinical practice by repeated intravitreal injection, though effective, increases the risk of possible complications, including an increase in intraocular pressure cataract, retinal detachment, endophthalmitis, and vitreous hemorrhage.[8–10]

Delivering to the posterior segment via the transscleral route is gaining popularity.[11–17] It is proximal to the retina and circumvents the corneal epithelium and the lens. The outermost barrier along the transscleral path, the sclera, is a hydrated fibrous network of collagen, elastin, and proteoglycan.[18] It is permeable to hydrophilic molecules and even large molecules such as dextran, protein, and nucleic acid.[19] However, the low scleral permeability to macromolecules, together with the dynamic clearance by uveoscleral outflow and episcleral circulation,[7] limits the utility of transscleral route for delivering therapeutics.

To increase the transscleral flux of macromolecules, we have proposed using ultrasound as a noninvasive approach to increase the permeability of sclera.[20] We found that short duration of low-frequency, low-intensity ultrasound enhanced the transport of dextran and albumin protein significantly across rabbit sclera in ex vivo experiments.[21,22] Here, we aim to provide evidence in live rabbits to support our hypothesis that ultrasound is an effective and noninvasive approach for transscleral delivery. The amount of macromolecular probe (70 kDa dextran) transported from the scleral surface to vitreous, with and without ultrasound treatment, was compared to assess the effect and duration of ultrasound. Electroretinography, binocular indirect microscopy (BIO), and histology were employed to evaluate whether there is any

negative impact of ultrasound on the visual function and integrity of posterior ocular tissues.

Methods

Materials

Fluorescein isothiocyanate labeled Dextran (FITC-Dextran; MW: 70 kDa; Sigma-Aldrich, St. Louis, MO) was used as the macromolecular probe. FITC-Dextran was dissolved in PBS solution to a final concentration of 1% (w/v) and is denoted as "dextran solution" hereinafter.

Animals

All the experimental and animal handling procedures were in accordance with the ARVO Statement for the Use of Animals in Ophthalmic and Vision Research. The use of animals was conducted according to the requirements of the Animals Ordinance (Control of Experiments; Cap. 340) and all relevant legislation and codes of practice in Hong Kong. All procedures were approved by the Faulty Committee on the Use of Live Animals in Teaching and Research at The University of Hong Kong (CULATR 2423–11) and The Hong Kong University of Science and Technology (APCF 2012010).

In Vivo Ultrasound Application

The rabbit was first anesthetized by injection with 2% xylazine (0.4 mL/kg) and 10% ketamine (0.45 mL/kg). Experiments were carried out within two hours after anesthetization. The ultrasound transducer was inserted into an adaptor containing either dextran solution or PBS, and placed in contact with the sclera at superior-temporal quadrant (approximately 5 mm behind the limbus; Fig. 1). This quadrant is chosen as the sonication zone due to its proximity to posterior segment and absence of extraocular muscle. The sonication zone has a radius of 2.5 mm.

A nonfocusing, double piezoceramics elements, planar transducer with a diameter of 45 mm operating at a center frequency of 40 kHz (Model CCH-4535D-40LB-PZT-4 ultrasound transducer; Beijing Cheng-cheng Weiye Science and Technology Co., Ltd., Beijing, People's Republic of China) generated the ultrasound field. The peak rarefactional pressure was measured in a water tank using a calibrated 9.5-mm hydrophone (model 8103 miniature hydrophone; Brüel & Kjær, Nærum, Denmark) and a conditioning amplifier (model 2691-A-0S2, 2-channel [single probe] intensity conditioning amplifier; Brüel & Kjær). The ultrasound transducer was driven by a signal from an arbitrary waveform generator (model GFG-8216A; Instek, Taipei, Taiwan). The signal generator was connected in series with an amplifier (Model 7500 Amplifier; Krohn-hite, Brockton, MA), then connected in series to the ultrasound transducers. An oscilloscope (TDS1002B; Tektronix, Beaverton, OR) was connected in parallel to the signal generator to monitor the input signal. The intensity of the ultrasound was calibrated using calorimetric method similar to Zderic et al.[23] Details of calorimetric method are provided in the Supplementary Material.

A cycle of sonication process consists of two steps. First, continuous sonication with dextran solution (40 kHz for 90 seconds) inside the adaptor at acoustic power (I_{SATA}, spatial average–temporal average intensity) 0.12 W/cm^2 were delivered via the transscleral route. Second, after sonication, the dextran solution remained in contact with the sclera for 5 minutes. Steps 1 and 2 were repeated up to a total of three cycles in experiments. The ultrasound parameters here corresponded to a mechanical index (MI)[24] of 0.20. (The definition of MI is shown in the Supplementary Material.) Scleral surface temperature before and after ultrasound application were measured by a thermocouple (206-3738; RS Components Ltd., Hong Kong, China). Vitreous was extracted for fluorescence detection within 10 minutes. The control group was done without placing ultrasound transducer above the eye.

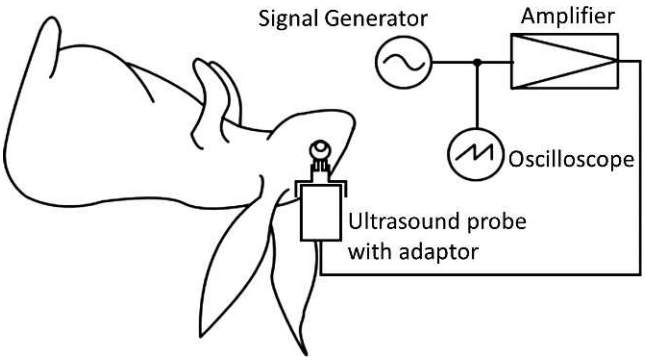

Figure 1. Graphical illustration of the in vivo experiment setup.

For the sclera recovery experiment, PBS solution was used to fill the adaptor during ultrasound application. A continuous ultrasound wave at 40 kHz and 0.12 W/cm^2 was applied to the eye for 90 seconds three times, with a break of 5 minutes between each time. After a lag time of 1 day, 7 days, and 14 days, dextran solution was placed in contact with the sclera around the sonication zone for 15 minutes. The vitreous was extracted for fluorescence detection. At the same time points, BIO, ffERG, and a histological examination were performed. A schematic diagram for in vivo experiments is shown in Figure 2.

Vitreous Fluorescence Measurement

After removal of periocular tissues (conjunctiva, muscles, and orbital fat), vitreous was extracted according to procedures reported by Enea et al., with modification.[25] Briefly, the aqueous humor was aspirated with a 29-gauge needle inserted through the cornea into the anterior chamber of the eye. The eye was cut open with a razor blade and the lens was removed with a pair of forceps. The vitreous body was carefully obtained after removing all attached retinal tissue and weighed. The vitreous body was homogenized by vortexing in the presence of steel beads. The homogenate was centrifuged at 4500 rpm for 5 minutes. The supernatant was sampled and the fluorescence intensity was measured using a spectrofluorometer (Wallac VICTOR^3 1420 Multilabel Counter; Perkin Elmer, Waltham, MA; excitation: 485 nm, emission: 535 nm) in a 96-well plate. The experiments were conducted in triplicates with three different rabbit eyes. Fluorescence intensity was converted to equivalent FITC-dextran concentration in vitreous by calibration to a standard curve constructed with serial dilution of 10 μL FITC-dextran in 190 μL homogenized vitreous from untreated rabbit eye. The lower detection limit of the assay is 0.0032 μg FITC-dextran/g vitreous.

Electroretinography

Dark- and light-adapted full-field electroretinogram (ffERG; PS33-PLUS; Natus Neurology, Inc., Warwick, RI) were recorded at 4 days before as well as 1 day, 7 day, and 14 days after ultrasound treatment. Before ffERG recording, rabbits were anesthetized as indicated in the earlier description. The cornea

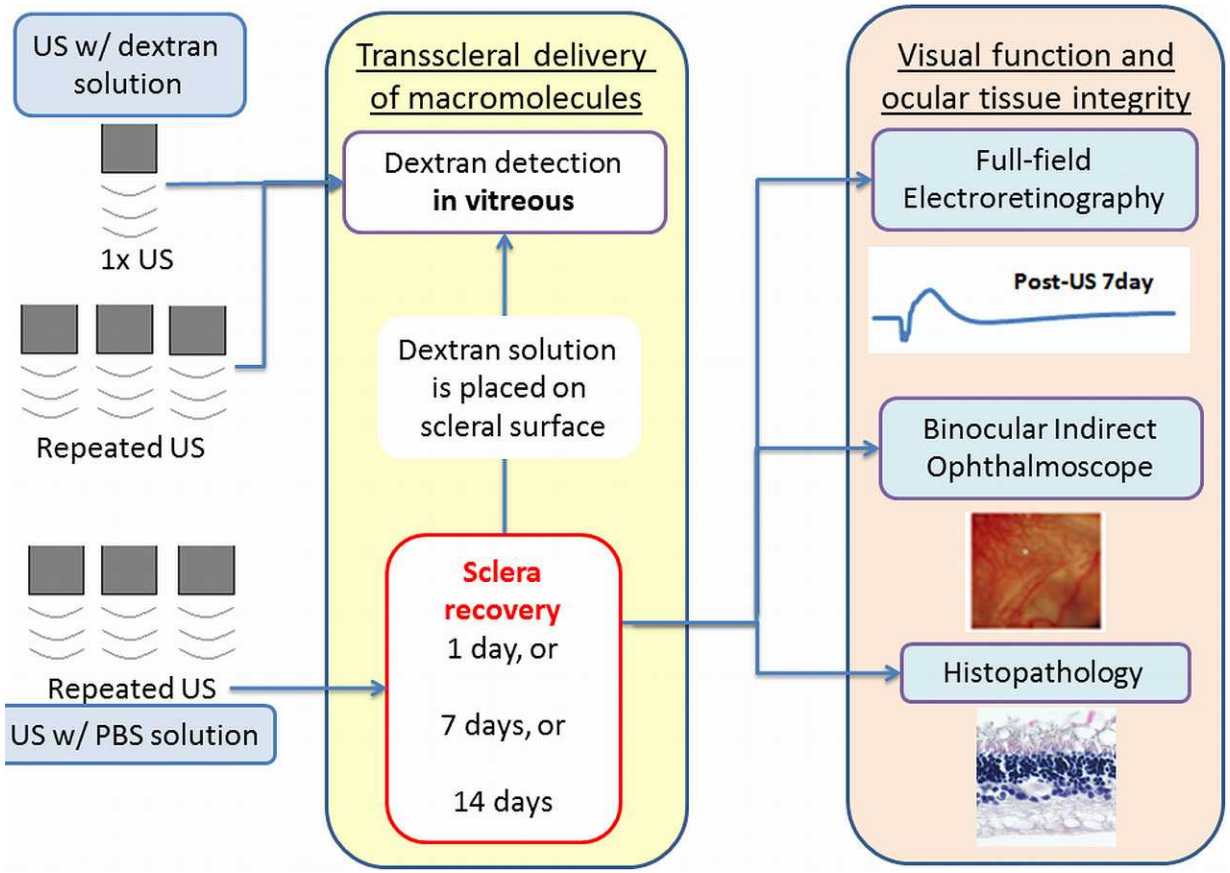

FIGURE 2. Schematic diagram of experimental design.

was anesthetized with 1 drop of 0.5% propavacaine HCl and the pupils were dilated to a diameter of 8 to 9 mm with two drops of 1% tropicamide. ERG signals were recorded by a unipolar corneal electrode (ERG-jet; Fabrinal, La Chaux-de-Fonds, Switzerland), reference electrode inserted into the eyelid with the ground electrode inserted into the ear. Animals were dark-adapted for 20 minutes before stimulation with a single, full-field white light flash (10 μs, 5.5 lumen s/ft^2) delivered every 35 seconds for dark-adapted ERG. In light-adapted ERG, animals were stimulated with single full-field white light flash (10 μs, 5.5 lumen s/ft^2) delivered every 15 seconds. The ERG signals were amplified at 20,000 gain and filtered between 1 to 300 Hz by amplifier (CP511 A.C. amplifier; Natus Neurology, Inc.). Approximately 28 responses were recorded. The amplitude of a-wave of ERG was measured from the baseline to the trough, and that of b-wave was measured from the trough of the a-wave to the peak of b-wave. Measured amplitudes of a- and b-wave were normalized as below:

Normalized Amplitude = Wave Amplitude (1d, 7d, or 14d post-US)/Wave Amplitude (pre-US).

Binocular Indirect Ophthalmoscopy

Rabbit and cornea were anesthetized as described earlier, except that two drops of 1% tropicamide HCl were given to dilate the pupils. BIO was taken using a commercial microscope (digital binocular indirect microscope, Keeler Vantage Plus Digital, 1205-P-5010; Keeler Ltd., London, UK).

Histologic Analysis

Ultrasound-treated ($n = 7$) and unoperated ($n = 4$) rabbits were humanely killed by intravenous injection of 1.5 mL sodium pentobarbital into the marginal ear veins. The left eyes were enucleated and fixed with 4% paraformaldehyde overnight. The globes were then cut into two eyecups. The eyecups containing the ultrasound-treated areas were further dehydrated in graded series of alcohol and chloroform, followed by paraffin embedding. Sections of 7 μm around the ultrasound-treated areas were cut with a microtome (Microm HM 315R; Heidelberg Engineering, Heidelberg, Germany). Sections at the ultrasound-treated area (behind limbus, superior-temporal quadrant) were selected, stained with hematoxylin and eosin (H&E), and examined under a light microscope at ×100 and ×400 magnification (Eclipse 80i; Nikon Instruments, Inc., Tokyo, Japan). Photographs were taken with a digital camera (SPOT RT3; Diagnostic Instruments, Inc., Sterling Heights, MI). Similarly, corresponding regions in the un-operated eyes were processed and imaged. In each eye, thickness of outer nuclear layer (ONL), total retina and sclera at the ultrasound treated region were measured. A total of 25 measurements (5 measurements in 5 separate sections) from each sectioned eye were taken and averaged. Two eyes from the ultrasound-treated group were rejected due to artificial retinal detachment and folding.

Statistics

Data were presented as mean ± SD. Unpaired *t*-test, one-way ANOVA, and Bonferroni's multiple comparison tests were

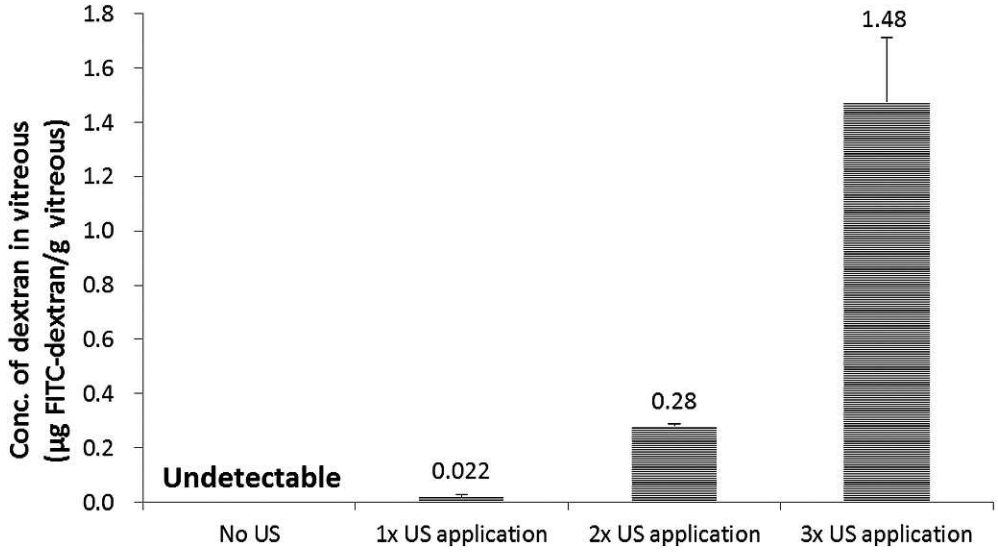

FIGURE 3. Effect of ultrasound applications on transscleral delivery of macromolecules in vivo 70 kDa dextran ($n = 3$). The difference between any two groups shown is statistically significant ($P < 0.05$, unpaired two-tailed Student's *t*-test). US, ultrasound.

used for comparison of results as specified in the Figures 3, 4, and 6 legends (Prism 5.0; GraphPad Software, Inc., San Diego, CA). A statistically significant difference was stated when $P < 0.05$.

RESULTS

Ultrasound-Enhanced Transscleral Delivery of Macromolecules

Ultrasound application on the sclera surface enhanced the amount of macromolecules transported transsclerally (Fig. 3). Without ultrasound treatment, dextran applied on the sclera surface could not be detected inside the vitreous. After one ultrasound application of 90 seconds, the concentration rose to 0.022 µg FITC-dextran/g of vitreous. The concentration increased nonlinearly with the repeat of sonication. Triple sonication resulted in a further 70-fold increase in dextran concentration inside the vitreous compared with single sonication. We monitored the temperature on the surface of the rabbit eye during and after ultrasound application. The temperature rise was negligible in all experiments.

Duration of Ultrasound Enhancement

Transscleral barrier against dextran transport was restored to normal approximately 2 weeks after multiple sonication (Table). When dextran was applied on the sclera 7 days after ultrasound treatment, the probe concentration found in vitreous was significantly lower than the case with zero lag time. When the lag time was increased to 14 days, dextran could not be detected inside vitreous, comparable with the observation in control without ultrasound treatment.

TABLE. Concentration of Dextran in Vitreous

Lag Time of Dextran Application Post-US Applications, 3×	Concentration of FITC-Dextran in Vitreous, µg/g vitreous
t = 0	1.48 ± 0.24
t = 7 d	0.024 ± 0.002
t = 14 d	Below detection limit
Control, no US application	Below detection limit

Dextran solution was applied after indicated lag time following three ultrasound applications, with 5 minutes spaced between each. Dextran solution remained in contact with sclera for 15 minutes ($n = 3$).

Electroretinography

After ultrasound application, normalized amplitude of a- and b-wave from light- and dark-adapted ERG experiments showed values around unity, and no statistical significance is found between preultrasound and postultrasound-treated groups. There was also no difference among groups at different lag times (one-way ANOVA and Bonferroni's multiple comparison test, $P = 0.28$; Fig. 4).

Binocular Indirect Ophthalmoscopy

BIO images of peripheral area and regions near optic disc of ultrasound-treated eyes showed no severe structure alteration. No significant change in the structure of retina and choroid of the ultrasound-treated rabbit was observed. No hemorrhage, retinal detachment, edema, neovascularization, or any other damage was observed after ultrasound applications up to 14 days.

Histology of Ocular Tissues

The thickness of the ONL, total retina, and sclera was measured and compared between the unoperated and ultrasound-treated eyes. There was no statistically significant difference in the thickness of ONL ($P = 0.56$); total retina ($P = 0.32$); and sclera ($P = 0.99$, unpaired I-test) between unoperated and ultrasound-treated eyes (Fig. 5).

Sections of the eyes at the ultrasound application site were also examined and compared between unoperated and ultrasound-treated groups (Fig. 6). In both groups, all layers of the retina were present and no thinning or swelling was observed. Cells appeared normal with no pyknotic or condensed nuclei, suggesting absence of cell death. In the sclera of unoperated eyes, fibers were arranged in bundles parallel to the surface. Similarly, the sclera of the ultrasound-treated eyes showed no significant difference.

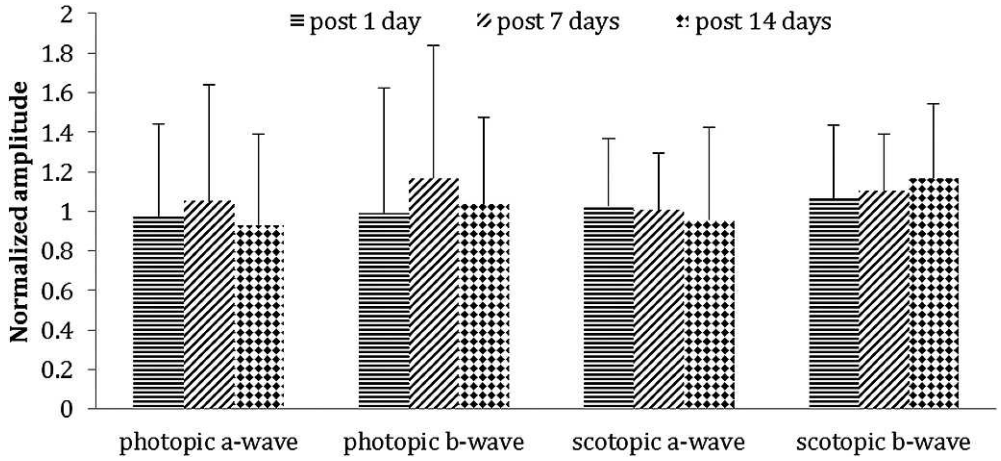

FIGURE 4. Normalized a- and b- waves of photopic and scotopic ffERG 1 day, 7 days, and 14 days after ultrasound applications ($n = 5$ in each group). Results are normalized by pre-US value. For each wave type, no statistical significance among different time points is found using one-way ANOVA test and Bonferroni's multiple comparison tests.

DISCUSSION

Herein, we demonstrate effective delivery of macromolecules to rabbit eye in vivo by low frequency and low intensity ultrasound. No undesirable effects were found on visual function and ocular tissue integrity. The results highlight the potential of a noninvasive approach to deliver high molecular weight therapeutics to the back of the eye.

The data here support that ultrasound increases the inward flux of large molecules to an extent that overcomes the static and dynamic barriers in the transscleral route of delivery. Structurally, the barriers include sclera, choroid, brunch's membrane, and retinal pigment epithelium. Molecules may also be cleared by the blood flow of episclera and choroid, the lymphatic vessels, as well as the outward fluid flow due to intraocular pressure.[26] Passive diffusion of macromolecules across tissue barriers is even slower because of its large size.[7] Many important therapeutics for posterior eye diseases are biomacromolecules (e.g., bevacizumab at 149 kDa, ranibizumab at 48 kDa, pegaptanib at 50 kDa, and aflibercept at 97 kDa).[3,5,27] Although protein and DNA are permeable across sclera—the outmost hydrophilic barrier in the transscleral route—the diffusivity is relatively low.[19,28] This property on top of the dynamic clearance makes it challenging for macromolecules topically applied on the sclera to be transported to the posterior segment.[29] This is consistent with our observation in the control experiment with the macromolecular probe, FITC-dextran of 70 kDa. The level found in vitreous is below the detectable limit (Fig. 3). A single sonication cycle at the chosen parameters was capable of overcoming the transscleral barrier to deliver a detectable amount of dextran into the vitreous. Notably, repeating the number of sonication cycles, there is a dramatic, nonlinear enhancement in the effectiveness of delivery. The concentration of macromolecular probe found in vitreous was at a range that, when applied to protein therapeutic, is sufficient to produce biological effects.[3,30,31] Further investigations on ultrasound-enhanced delivery of therapeutics will be required to optimize and establish if the enhancement is sufficient for clinical applications.

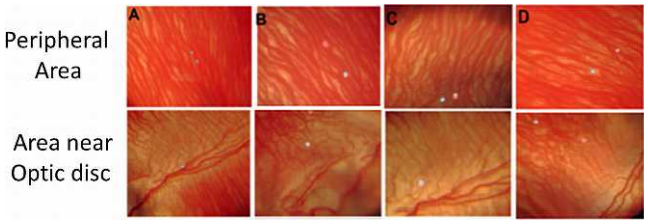

FIGURE 5. Representative BIO images of rabbit retina-choroid. (**A**) Before US application. (**B**) 1 day post-US application. (**C**) 7 days post-US application. (**D**) 14 days post-US application.

In our study, the control group was done without placing ultrasound transducer above the eye. A custom-made adapter containing aqueous solution was placed between the ultrasound probe and the sclera surface to enable the transmission of ultrasound. This also means that there is no direct contact of the ultrasound probe and the scleral surface, so that the mechanical force exerted by the probe in the absence of ultrasound is negligible. The lack of effect by probe action alone was also supported by our previous observation that ultrasound applied at high frequency resulted in no enhancement of intrascleral penetration by macromolecules.[20] On the other hand, the effect on the transscleral delivery depends on the variation in ultrasound parameters.[21,22]

The choice of low frequency in this study was based on previous results from our group, showing that transscleral penetration of macromolecules increases with decreasing frequency.[20,32] The acoustic intensity used was far below the value used in transdermal delivery[33,34] and cancer-targeted delivery.[35–37] Measuring the peak rarefaction pressure at this low intensity (I_{SATA}: 0.12 W/cm^2) enabled us to calculate the MI (Supplementary Material). As the name suggests, MI is a measure of the mechanical effect of ultrasound. For safety reasons, the upper limit of MI was set up by US Food and Drug Administration and The American Institute of Ultrasound in Medicine (AIUM).[38] Although there is no direct guideline to ocular drug delivery, the MI limit for ophthalmic diagnosis is 0.23. MI of experiments in this report was 0.20, which is well below the regulatory limit previously mentioned. The regulatory agency also imposes a control on the temperature rise by ultrasound, recommending the thermal index (TI) to be below 1.0.[39] (The calculation of TI is shown in the Supplementary Material.) Because of the low acoustic intensity and the short duration time in each cycle, temperature rise was negligible. Therefore, the ultrasound parameters in this study are chosen after considering both delivery efficiency and safety guideline.

While ultrasound enhances transscleral delivery, the window of effective delivery must be temporary for the method to be deemed noninvasive. The barrier against the entry of

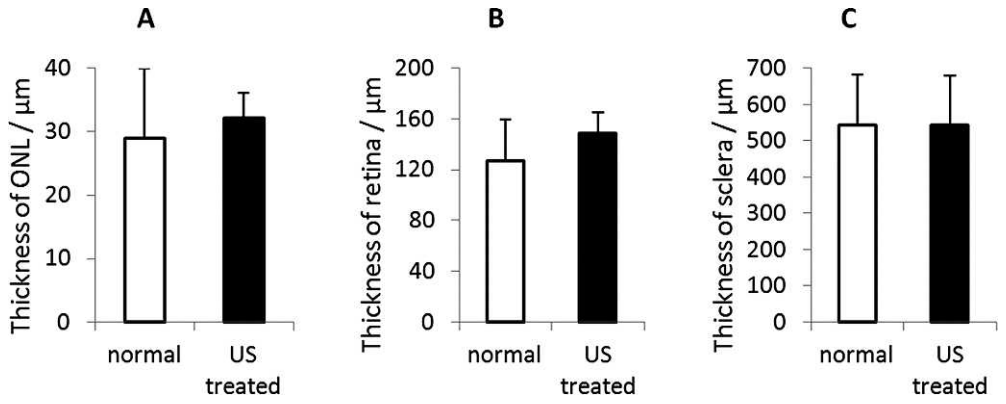

FIGURE 6. Thicknesses comparison of the ONL, retina, and sclera in unoperated and ultrasound-treated rabbit eyes. (**A**) ONL thickness, normal ($n = 4$) = 28.9 ± 11.1 µm ($n = 4$); US treated ($n = 5$) = 32.1 ± 4.1 µm ($n = 5$), $P = 0.56$. (**B**) Total retina thickness, normal = 126.7 ± 33.1 µm ($n = 4$); US treated = 148.6 ± 17.0 µm ($n = 5$). (**C**) Sclera thickness, normal = 544.1 ± 139.1 µm ($n = 4$); US treated = 543.2 ± 137.6 µm ($n = 7$). No significant difference was observed in thickness of ONL, retina, and sclera between the unoperated and US-treated eyes (one-way ANOVA Test and Bonferroni's Multiple comparison test).

nonindigenous substance must be weakened, but only for a short period of time, in order to balance with the risk of infection. The transscleral barrier showed a gradual healing process over 14 days after sonication (Table). By the end of this period, the macromolecular probe could not be detected in the vitreous, supporting the "opening" created by ultrasound was not permanent. The restoration property is crucial in future clinical application because scleral barrier has to reseal for eye protection. After intravitreal injection, the needle hole in conjunctiva and sclera requires several days to heal and water-seal.[40] Evaluation of the duration of ultrasound effect is only one aspect in addressing safety issues that may arise from the new approach. We examined the ultrasound-treated eye with three complementary techniques to assess if any side effect is produced on ocular tissue structure and visual function.

Full-field electroretinography provides insight into the global electrical response of retina to photic stimulation. Results indicated that the ultrasound did not affect either the cone or the rod system (Fig. 4). Two key parameters were extracted in ffERG analysis: the amplitude from baseline to the trough of a-wave and the amplitude of b-wave from trough of a-wave to the peak of b-wave. A-wave is contributed by photoreceptors and reflects the physiological condition of photoreceptors.[41–43] B-wave is contributed by the secondary sensory neurons, mainly by on-center bipolar cells and Müller cells.[44] If the photoreceptors are damaged, the a-wave will be affected, and hence the b-wave; if the signal transduction from photoreceptors to bipolar cells is affected or the bipolar cells are damaged, an abnormal b-wave will occur. For the photopic ERG, since the rods are bleached by bright light, the ERG signals are contributed by cone systems. For the scotopic ERG, since the rods are much more sensitive than cones in a dark environment, the ERG signals are mainly contributed by rod system after a dark adaptation. We found no significant change, neither short-term (1 day) nor long-term (14 days), in the amplitude of a- and b-waves of photopic and scotopic ERG after US. The waveforms of photopic and scotopic ERG at all the time points sampled did not show any abnormality (Supplementary Material), further supporting that ultrasound at the chosen parameters did not influence the electrical response of retinal cells upon photic stimulation.

Ocular tissue was examined by BIO for macroscopic images, and then by histology for microscopic morphology. No damage was found. BIO images indicated that the overall structure of the posterior segment of the treated rabbit eyes remained intact. No gross damage such as hemorrhage, edema, or neovascularization was noted up to 14 days after ultrasound application (Fig. 5). Microscopically, the overall morphology of the retina and sclera of ultrasound-treated eyes was not found to be modified when compared with unoperated eyes under ×100 and ×400 magnification (Fig. 7). In the sections, retinal ganglion cells appeared to be absent in the ganglion cell layer of the retina. This can be explained by the finding that the distribution of ganglion cells at superior peripheral retina near the ora serrata is low, at only approximately 800 cells/mm^2.[45,46] The thickness of the sclera or retina is an indication of the integrity of the layer, as any damage to the sclera or retina would lead to cell death and shrinkage of the layer (Fig. 6). The observed unchanged thickness of sclera and retina suggests that the sclera and retina is not disrupted by ultrasound treatment. We further measured the thickness of the ONL as ONL is comprised of cell bodies of the photoreceptors (Fig. 6). The observation that ONL thickness was not significantly changed after ultrasound treatment was

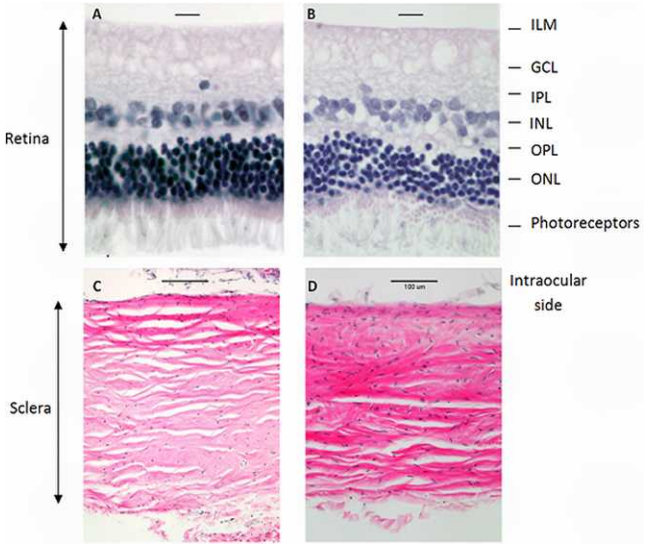

FIGURE 7. H&E staining of H&E-stained cross sections of the area behind the limbus in superior-temporal quadrant of rabbit left eyes. (**A**) Retina, normal unoperated. (**B**) Retina, US-treated, scale represents 210 µm. (**C**) Sclera, normal unoperated. (**D**) Sclera, US-treated. There was no obvious change in the gross structure of the retina and sclera after ultrasound administration. *Scale bars*: = 10 µm (**A**, **B**), 100 µm (**C**, **D**).

consistent with the unaffected a-wave amplitude, further supporting that the ultrasound treatment causes no significant change to the structure of the posterior segment of the eye.

Conclusions

This study showed for the first time that it is feasible to use low-frequency, low-intensity ultrasound to deliver macromolecules into posterior segments of the eye via the transscleral route. Transscleral barriers were found to be restored 2 weeks postultrasound application. Electric response of retinal cells remained intact and no structural or morphological changes in the ocular tissues were observed after sonication. Hence, the results support the potential of ultrasound as a noninvasive approach for delivering therapeutics transsclerally to the back of the eye.

Acknowledgments

We thank Chi Wai Wong for providing technical support in the electroretinography study.

Supported by the Innovation and Technology Fund and Research Grants Council of the Hong Kong Government.

Disclosure: **W.-L.L. Suen**, None; **H.S. Wong**, None; **Y. Yu**, None; **L.C.M. Lau**, None; **A.C.-Y. Lo**, None; **Y. Chau**, None

References

1. World Health Organization. Prevention of blindness and visual impairment: Priority eye diseases—Age related macular degeneration. Available at: http://www.who.int/blindness/causes/priority/en/index8.html. Accessed January 20, 2013.
2. Ohr M, Kaiser PK. Intravitreal aflibercept injection for neovascular (wet) age-related macular degeneration. *Expert Opin Pharmacother*. 2012;13:585–591.
3. Moshfeghi AA, Puliafito CA. Pegaptanib sodium for the treatment of neovascular age-related macular degeneration. *Expert Opin Investig Drugs*. 2005;14:671–682.
4. Schmucker C, Ehlken C, Hansen LL, Antes G, Agostini HT, Lelgemann M. Intravitreal bevacizumab (Avastin) vs. ranibizumab (Lucentis) for the treatment of age-related macular degeneration: a systematic review. *Current Opin Ophthalmol*. 2010;21:218–226.
5. Schmucker C, Loke YK, Ehlken C, et al. Intravitreal bevacizumab (Avastin) versus ranibizumab (Lucentis) for the treatment of age-related macular degeneration: a safety review. *Br J Ophthalmol*. 2011;95:308–317.
6. Zhang K, Hopkins JJ, Heier JS, et al. Ciliary neurotrophic factor delivered by encapsulated cell intraocular implants for treatment of geographic atrophy in age-related macular degeneration. *Proc Natl Acad Sci U S A*. 2011;108:6241–6245.
7. Ambati J, Canakis CS, Miller JW, et al. Diffusion of high molecular weight compounds through sclera. *Invest Ophthalmol Vis Sci*. 2000;41:1181–1185.
8. Jonas JB, Kreissig I, Degenring R. Intraocular pressure after intravitreal injection of triamcinolone acetonide. *Br J Ophthalmol*. 2003;87:24–27.
9. Wu L, Martinez-Castellanos MA, Quiroz-Mercado H, et al. Twelve-month safety of intravitreal injections of bevacizumab (Avastin): results of the Pan-American Collaborative Retina Study Group (PACORES). *Graefes Arch Clin Exp Ophthalmol*. 2008;246:81–87.
10. Sonmez K, Ozturk F. Complications of intravitreal triamcinolone acetonide for macular edema and predictive factors for intraocular pressure elevation. *Int J Ophthalmol*. 2012;5:719–725.
11. D.M. Maurice SM. Ocular pharmacokinetics. *Pharmacol Eye*. 1984;69:19–116.
12. Barza M. Antibacterial agents in the treatment of ocular infections. *Infect Dis Clin North Am*. 1989;3:533–551.
13. Raghava S, Hammond M, Kompella UB. Periocular routes for retinal drug delivery. *Expert Opin Drug Deliv*. 2004;1:99–114.
14. Ranta VP, Urtti A. Transscleral drug delivery to the posterior eye: prospects of pharmacokinetic modeling. *Adv Drug Deliv Rev*. 2006;58:1164–1181.
15. Geroski DH, Edelhauser HF. Transscleral drug delivery for posterior segment disease. *Advanced Drug Deliv Rev*. 2001;52:37–48.
16. Lee SJ, He W, Robinson SB, Robinson MR, Csaky KG, Kim H. Evaluation of clearance mechanisms with transscleral drug delivery. *Invest Ophthalmol Vis Sci*. 2010;51:5205–5212.
17. Paganelli F, Cardillo JA, Dare AR, et al. Controlled transscleral drug delivery formulations to the eye: establishing new concepts and paradigms in ocular anti-inflammatory therapeutics and antibacterial prophylaxis. *Expert Opin Drug Deliv*. 2010;7:955–965.
18. Watson PG, Young RD. Scleral structure, organisation and disease. A review. *Exp Eye Res*. 2004;78:609–623.
19. Prausnitz MR, Noonan JS. Permeability of cornea, sclera, and conjunctiva: a literature analysis for drug delivery to the eye. *J Pharm Sci*. 1998;87:1479–1488.
20. Cheung AC, Yu Y, Tay D, Wong HS, Ellis-Behnke R, Chau Y. Ultrasound-enhanced intrascleral delivery of protein. *Int J Pharm*. 2010;401:16–24.
21. Chau Y. Enhancement of transscleral transport of macromolecules by sonophoresis. Presented at: 38th Annual Meeting & Exposition of the Controlled Release Society; August 2011; National Harbor, MD.
22. Wong H-S. Ultrasound-Mediated Transscleral Drug Delivery. Hong Kong, China: Department of Chemical and Biomolecular Engineering: The Hong Kong University of Science and Technology. 2011;89.
23. Zderic V, Vaezy S, Martin RW, Clark JI. Ocular drug delivery using 20-kHz ultrasound. *Ultrasound Med Biol*. 2002;28:823–829.
24. Szabo TL. *Diagnostic Ultrasound Imaging: Inside Out*. Waltham: Academic Press; 2004:576.
25. Enea NA, Hollis TM, Kern JA, Gardner TW. Histamine H1 receptors mediate increased blood-retinal barrier permeability in experimental diabetes. *Arch Ophthalmol*. 1989;107:270–274.
26. Kim SH, Lutz RJ, Wang NS, Robinson MR. Transport barriers in transscleral drug delivery for retinal diseases. *Ophthalmic Res*. 2007;39:244–254.
27. Heier JS, Brown DM, Chong V, et al. Intravitreal aflibercept (VEGF trap-eye) in wet age-related macular degeneration. *Ophthalmology*. 2012;119:2537–2548.
28. Shuler RK Jr, Dioguardi PK, Henjy C, Nickerson JM, Cruysberg LP, Edelhauser HF. Scleral permeability of a small, single-stranded oligonucleotide. *J Ocul Pharmacol Ther*. 2004;20:159–168.
29. Ottiger M, Thiel MA, Feige U, Lichtlen P, Urech DM. Efficient intraocular penetration of topical anti-TNF-alpha single-chain antibody (ESBA105) to anterior and posterior segment without penetration enhancer. *Invest Ophthalmol Vis Sci*. 2009;50:779–786.
30. Gaudreault J, Fei D, Beyer JC, et al. Pharmacokinetics and retinal distribution of ranibizumab, a humanized antibody fragment directed against VEGF-A, following intravitreal administration in rabbits. *Retina*. 2007;27:1260–1266.
31. Krohne TU, Eter N, Holz FG, Meyer CH. Intraocular pharmacokinetics of bevacizumab after a single intravitreal injection in humans. *Am J Ophthalmol*. 2008;146:508–512.

Investigative Ophthalmology & Visual Science

32. Chau Y, Tse HY. Investigation of the mechanism of ultrasound-enhanced transscleral transport of macromolecules. Presented at: 2011 American Institute of Chemical Engineers Annual Meeting; October 2011; Minneapolis, MN.
33. Tang H, Blankschtein D, Langer R. Effects of low-frequency ultrasound on the transdermal permeation of mannitol: comparative studies with in vivo and in vitro skin. *J Pharm Sci*. 2002;91:1776–1794.
34. Tezel A, Mitragotri S. Interactions of inertial cavitation bubbles with stratum corneum lipid bilayers during low-frequency sonophoresis. *Biophys J*. 2003;85:3502–3512.
35. Park EJ, Zhang YZ, Vykhodtseva N, McDannold N. Ultrasound-mediated blood-brain/blood-tumor barrier disruption improves outcomes with trastuzumab in a breast cancer brain metastasis model. *J Control Release*. 2012;163:277–284.
36. Husseini GA, Pitt WG. Ultrasonic-activated micellar drug delivery for cancer treatment. *J Pharm Sci*. 2009;98:795–811.
37. Schroeder A, Honen R, Turjeman K, Gabizon A, Kost J, Barenholz Y. Ultrasound triggered release of cisplatin from liposomes in murine tumors. *J Control Release*. 2009;137:63–68.
38. O'Brien WD. Ultrasound-biophysics mechanisms. *Prog Biophys Mol Bio*. 2007;93:212–255.
39. Bigelow TA, Church CC, Sandstrom K, et al. The thermal index: its strengths, weaknesses, and proposed improvements. *J Ultrasound Med*. 2011;30:714–734.
40. Gomez-Ulla F, Basauri E, Arias L, Martinez-Sanz F. Management of intravitreal injections. *Arch Soc Esp Oftalmol*. 2009;84:377–388.
41. Brown KT. The electroretinogram: its components and their origin. *Vision Res*. 1968;8:633–777.
42. Brown KT, Murakami MA. New receptor potential of the monkey retina with no detectable latency. *Nature*. 1964;201:626–628.
43. Brown KT, Wiesel TN. Analysis of the intraretinal electroretinogram in the intact cat eye. *J Physiol*. 1961;158:229–256.
44. Dick E, Miller RF, Bloomfield S. Extracellular K+ activity changes related to electroretinogram components. II. Rabbit (E-type) retinas. *J Gen Physiol*. 1985;85:911–931.
45. Choudhury BP. Ganglion cell distribution in the albino rabbit's retina. *Exp Neurol*. 1981;72:638–644.
46. Oyster CW, Takahashi ES, Hurst DC. Density, soma size, and regional distribution of rabbit retinal ganglion cells. *J Neurosci*. 1981;1:1331–1346.

Investigative Ophthalmology & Visual Science